Experimental and Theoretical Studies on $Nb_4C_4^{0/+}$: Reactivity and Structure of the Smallest Cubic Niobium−Carbon Cluster

C. S. Yeh,† Y. G. Byun,† S. Afzaal,† S. Z. Kan,† S. Lee,† Ben S. Freiser,*,† and P. Jeffrey Hay*,‡

Contribution from the H. C. Brown Laboratory of Chemistry, Purdue University, West Lafayette, Indiana 47907, and Theoretical Division, T-12, MS B268, Los Alamos National Laboratory, Los Alamos, New Mexico 87545

Received September 21, 1994®

Abstract: $Nb_4C_4^+$, one of the smallest cubic crystallite structures (2×2×2) of the transition metal−carbon cluster family, is studied with the use of a Fourier transform ion cyclotron resonance (FT-ICR) mass spectrometer equipped with a compact supersonic source. $Nb_4C_4^+$ reacts with oxygen to form $Nb_4C_2^+$ and, presumably, 2CO. This reaction is analogous to that of $V_8C_{12}^+$ with O_2 in which $V_8C_{10}^+$ is produced. In contrast to the reaction of $V_8C_{12}^+$ with O_2, however, no higher order reactions are observed to proceed by elimination of one or two CO molecules. Taken together with other experiments, these results suggest that 8 eV < $D(Nb_4C_2^+-C_2)$ < 10 eV and $D(Nb_4^+-C_2)$ > 10 eV. In addition, this cluster ion is also found to react with both water and methanol through two competitive pathways which are dependent on the background Ar cooling gas. The main pathway for the cooled ions is attachment of the first solvent molecule followed by the elimination of H_2 upon reaction with the second solvent molecule to form $(OH)_2$ and $(OCH_3)_2$ adducts, respectively. A maximum of two additional solvent molecules then attach to the adduct ions. The reactions with water and methanol proceed with efficiencies of 3.9% and 2.7%, respectively. In the absence of cooling gas, abstraction to form $Nb_4C_4OH^+$ and $Nb_4C_4OCH_3^+$ from water and methanol, respectively, dominate and suggest $D(Nb_4C_4^+-OH) \leq D(H-OH)$ = 119 kcal/mol and $D(Nb_4C_4^+-OCH_3) \sim D(H-OCH_3)$ = 104 kcal/mol. Both of these product ions are observed to attach a maximum of 3 more solvent molecules at longer reaction times. *Ab initio* calculations are reported on Nb_4C_4 in a slightly distorted cubic structure with T_d symmetry. Calculations on Nb_4C_2 found one stable structure with essentially C_{2v} symmetry corresponding to a bicapped tetrahedron. The electronic structure of the ground and low-lying excited states is discussed as well as the observed reactivity of $Nb_4C_4^+$.

1. Introduction

Metal−carbon clusters have become the focus of intense investigation with the discovery of M_8C_{12} (M = Ti, V, Zr, and Hf), termed metallo-carbohedrenes or Met-Cars, as highly abundant "magic" peaks in mass spectra of metal−carbon clusters generated in a supersonic expansion.[1−5] Several structures have been proposed to account for the special stability of these ions.[6−15] Recently, we have reported evidence[16] which is consistent with the theoretically proposed low-energy T_d[8,9,15] or D_{2d}[10] structures, as opposed to the more symmetric T_h structure originally proposed.[1−5] Higher-order metal−carbon clusters have also been observed as especially abundant peaks.[3,17] Duncan and co-workers, for example, reported on $M_{14}C_{13}$ (M = Ti, V)[17] which, presumably, have face centered cubic unit cell structures similar to that of $Ti_{14}N_{13}$ titanium nitride nanocrystals[18] and alkali halide clusters.[19] Transition metal carbides in the bulk phase are also commonly known to crystallize in closely packed fcc lattices.[20]

For metal−carbon (metal = Ti, V, Nb) clusters, two types of stoichiometries are observed to be especially abundant, those corresponding to cubic crystallites (e.g., $M_{14}C_{13}$ and fragments such as M_nC_n, n = 4, 6, 9, etc.)[17,21,22] and metallo-carbohedrenes (M_8C_{12}).[1−5,21,22] Theoretical calculations performed by Reddy and Khanna have suggested that the relative concentrations of metal/carbon atoms during the condensation process influence

† Purdue University.
‡ Los Alamos National Laboratory.
® Abstract published in *Advance ACS Abstracts,* March 15, 1995.

(1) Guo, B. C.; Kerns, K. P.; Castleman, A. W. *Science* **1992**, *255*, 1411.
(2) Guo, B. C.; Wei, S.; Purnell, J.; Buzza, S.; Castleman, A. W. *Science* **1992**, *256*, 515.
(3) Wei, S.; Guo, B. C.; Purnell, J.; Buzza, S.; Castleman, A. W. *Science* **1992**, *256*, 818.
(4) Wei, S.; Guo, B. C.; Purnell, J.; Buzza, S.; Castleman, A. W. *J. Phys. Chem.* **1992**, *96*, 4166.
(5) Chen, Z. Y.; Guo, B. C.; May, B. D.; Cartier, S. F.; Castleman, A. W. *Chem. Phys. Lett.* **1992**, *198*, 118.
(6) Reddy, B. V.; Khanna, S. N.; Jena, P. *Science* **1992**, *258*, 1640.
(7) Hay, P. J. *J. Phys. Chem.* **1993**, *97*, 3081.
(8) Dance, I. *J. Chem. Soc., Chem. Commun.* **1992**, 1779.
(9) Lin, Z.; Hall, M. B. *J. Am. Chem. Soc.* **1993**, *115*, 11165.
(10) Chen, H.; Feyereisen, M.; Long, X. P.; Fitzgerald, G. *Phys. Rev. Lett.* **1993**, *71*, 1732.
(11) Pauling, L. *Proc. Natl. Acad. Sci. U.S.A.* **1992**, *89*, 8175.
(12) Rohmer, M. M.; De Vaal, P.; Benard, M. *J. Am. Chem. Soc.* **1992**, *114*, 9696.
(13) Gale, J. D.; Grimes, R. W. *J. Chem. Soc., Chem. Commun.* **1992**, 1222.
(14) Methfessel, M.; Van Schilfgaarde, M.; Scheffler, M. *Phys. Rev. Lett.* **1993**, *70*, 29.
(15) Rohmer, M. M.; Benard, M.; Henriet, C.; Bo, C.; Poblet, J. M. *J. Chem. Soc., Chem. Commun.* **1993**, 1182.
(16) Yeh, C. S.; Afzaal, S.; Lee, S.; Byun, Y. G.; Freiser, B. S. *J. Am. Chem. Soc.* **1994**, *116*, 8806.
(17) Pilgrim, J. S.; Duncan, M. A. *J. Am. Chem. Soc.* **1993**, *115*, 9724.
(18) Chen, Z. Y.; Castleman, A. W. *J. Chem. Phys.* **1993**, *98*, 231.
(19) (a) Martin, T. P.; Bergman, T.; Gohlich, H.; Lange, T. *J. Phys. Chem.* **1991**, *95*, 6421. (b) Beck, R. D.; St. John, P.; Homer, M. L.; Whetten, R. L. *Science* **1991**, *253*, 879.
(20) *Structural Inorganic Chemistry*; Wells, A. F., Ed.; Oxford, U. K., 1984; pp 947−953.
(21) Wei, S.; Guo, B. C.; Deng, H. T.; Kerns, K.; Purnell, J.; Castleman, A. W. *J. Am. Chem. Soc.* **1994**, *116*, 4475.
(22) Pilgrim, J. S.; Brock, L. R.; Duncan, M. A. *J. Phys. Chem.* **1995**, *99*, 544.

0002-7863/95/1517-4042$09.00/0

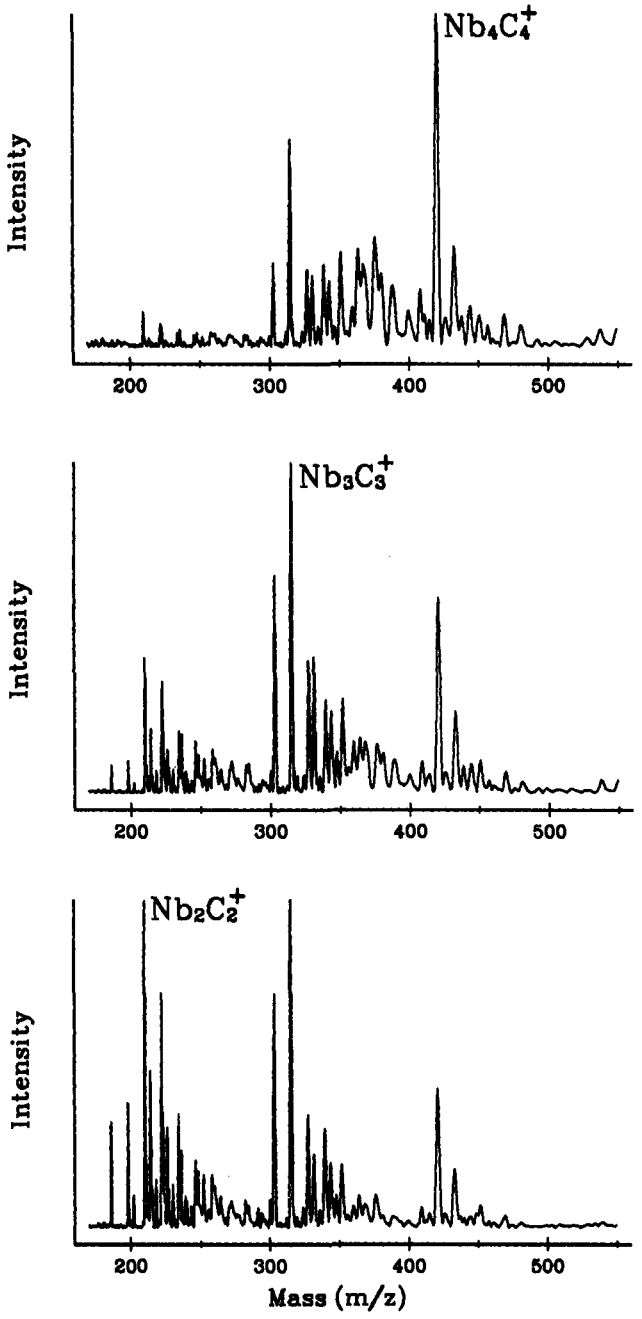

Figure 1. Mass spectra of niobium–carbon clusters acquired under otherwise identical conditions, except that the timing of the laser vaporization is changed with respect to the firing of the pulsed valve by an additional 2μs in each subsequent spectrum.

the formation of each cluster type.[23] Duncan's and Castleman's groups have both noted that the abundances of the two types strongly depend on experimental conditions and have discussed their formation in terms of thermodynamic and kinetic effects.[17,21,22]

In our experiments with niobium–carbon clusters, we have found $Nb_4C_4^+$, $Nb_3C_3^+$, and $Nb_2C_2^+$ to be the prominent ions in the mass spectrum below 450 daltons, as shown in Figure 1. Similar mass distributions have been observed by Castleman and Duncan. These species are also observed to be the dominant fragments in the photodissociation of higher-order niobium–carbon clusters.[22] Here, we report on the reactivity of $Nb_4C_4^+$ with oxygen, water, and methanol, along with its collision-induced dissociation. These results on $Nb_4C_4^+$, together with *ab initio* theoretical calculations on Nb_4C_4, support previous suggestions that these species have the form of a slightly distorted 2×2×2 cubic crystallite.

(23) Reddy, B. V.; Khanna, S. N. *Chem. Phys.* Lett. **1993**, *209*, 104.

2. Experimental Section

All experiments were performed on an Extrel (Millipore Corp., Madison, WI) FTMS-2000 dual cell Fourier transform ion cyclotron resonance (FT-ICR) mass spectrometer[24,25] combined with a compact supersonic source developed by Smalley and co-workers.[26] The laser vaporization technique is used to generate niobium–carbon clusters in a manner similar to Castleman and co-workers by seeding the He expansion gas with ~1% methane.[27–28] Frequency doubled 532 nm light from a Quanta Ray DCR Series 2 Nd:YAG laser is used for generating the metal plasma. The laser pulse occurs just prior to the arrival of a high-pressure burst of helium from a Jordan PSV pulsed valve. $Nb_4C_4^+$ predominates at lower laser powers (~15 mJ/pulse) and lower nozzle backing pressures (65 psi) than those used to generate $Nb_8C_{12}^+$ in our instrument. The laser has a 10 ns pulse width, and is focussed down to a ~0.5 mm diameter spot. The carrier gas and niobium mixture undergoes a supersonic expansion into a vacuum chamber pumped by a Balzers 300 L/s turbopump. The pressure of the source is maintained at $\sim 10^{-7}$ Torr. The ions then enter into the vacuum chamber (background pressure is $\sim 10^{-8}$ Torr) through a nickel skimmer where they pass down the axis of a stainless steel screen deceleration tube (40 cm length and 5 cm diameter). When the ions are about to emerge from the tube, the potential of the tube is lowered from 0 V to betweeen −50 and −80 V, depending on the mass of the ion being studied. The ions are decelerated due to the electric field between the end of the deceleration tube and the trapping plate of the analyzer side of the dual cell. The potential of the trapping plate is dropped from 9.81 to 4.5 V to allow the decelerated ions to enter the analyzer side of the dual cell. The potential is then raised back to its original value for the duration of the experiment. Good signals are obtained by accumulating ions generated from 10 pulses of the supersonic source.

Reagents are either introduced at a static pressure ($\sim 10^{-8}$–10^{-6} Torr) using Varian leak valves or pulsed into the vacuum chamber using General Valve Corporation Series 9 solenoid pulsed valves.[29] Argon is used as the collision gas at a static pressure of $\sim 2.9 \times 10^{-5}$ Torr. The $Nb_4C_4^+$ ions are collisionally cooled for several hundred milliseconds prior to isolation. Ion isolation[24] and collision-induced dissociation (CID)[30] are accomplished either by using standard FT-ICR radiofrequency pulses of variable frequency and power or by using SWIFT excitation.[31] For the rate constant measurements, Ar cooling gas was present at $\sim 2.9 \times 10^{-5}$ Torr and the water and methanol pressures were measured using standard procedures for calibrating the ion gauge for the sensitivity toward water and methanol.[32]

3. Details of the Calculations

Calculations were carried out at the Hartree–Fock level for Nb_4C_4 and Nb_4C_2 using a relativistic effective core potential[33] (ECP2) for Nb which replaces the inner electrons of the Nb atom and explicitly treats the "outer core" $4s^2\ 4p^6$ and valence shell $5s^1\ 4d^4$ electrons in the calculations. A "double-ζ" valence basis set was employed on Nb (DZ/ECP2) and C (6-31G), resulting in a contracted Gaussian basis of [3s3p2d] and [3s2p] for Nb and C, respectively. Calculations were carried out on closed-shell electronic states at the Hartree–Fock level.

(24) Cody, R. B.; Kissinger, J. A.; Ghaderi, S.; Amster, J. I.; McLafferty, F. W.; Brown, C. E. *Anal. Chim. Acta* **1985**, *178*, 43.
(25) Gord, J. R.; Freiser, B. S. *Anal. Chim. Acta* **1989**, *225*, 11.
(26) Maruyama, S.; Anderson, L. R.; Smalley, R. E. *Rev. Sci. Instrum.* **1990**, *61*, 3686.
(27) Guo, B. C.; Wei, S.; Chen, Z.; Kerns, K. P.; Purnell, J.; Buzza, S.; Castleman, A. W. *J. Chem. Phys.* **1992**, *97*, 5243.
(28) Chen, Z. Y.; Guo, B. C.; May, B. D.; Carteir, S. F.; Castleman, A. W. *Chem. Phys. Lett.* **1992**, *198*, 118.
(29) Carlin, T. J.; Freiser, B. S. *Anal. Chem.* **1983**, *55*, 571.
(30) (a) Cody, R. B.; Freiser, B. S. *Int. J. Mass Spectrom. Ion Phys.* **1982**, *41*, 199. (b) Cody, R. B.; Burnier, R. C.; Freiser, B. S. *Anal. Chem.* **1982**, *52*, 96.
(31) Wang, R. C. L.; Ricca, R. L.; Marshall, A. G. *Anal. Chem.* **1986**, *58*, 2935.
(32) Bartmess, J. E.; Georgiadis, R. M. *Vacuum* **1983**, *33*, 149.
(33) Hay, P. J.; Wadt, W. R. *J. Chem. Phys.* **1985**, *82*, 299.

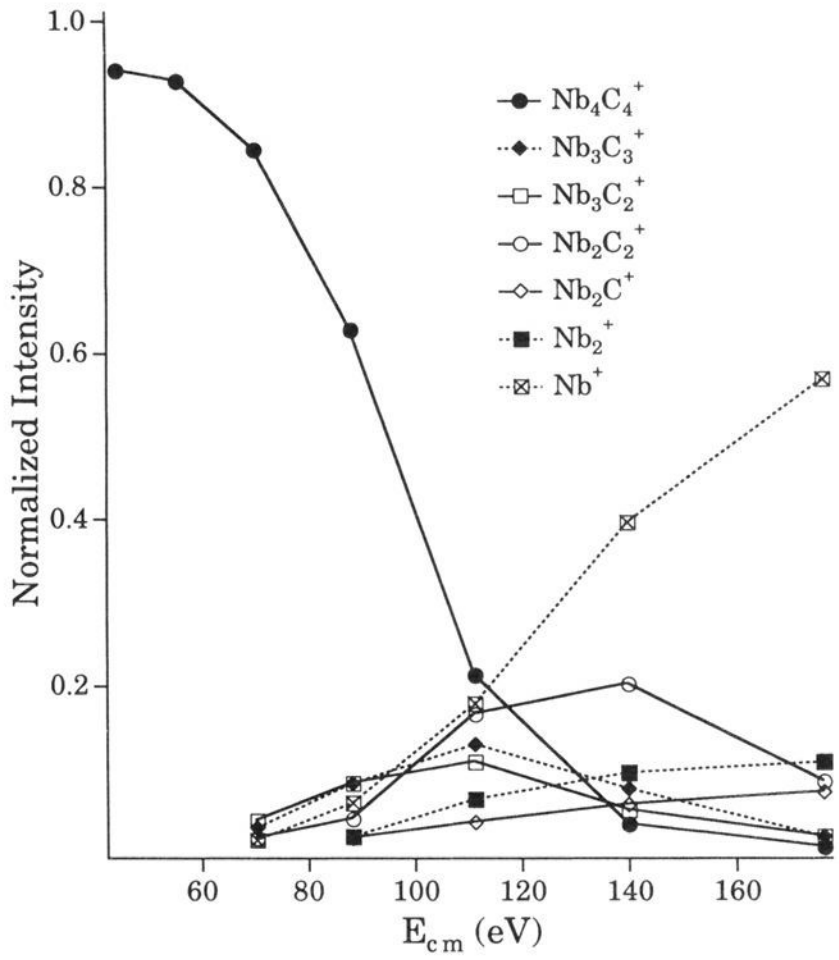

Figure 2. Energy-resolved CID plot of $Nb_4C_4^+$ under single-excitation conditions.

Restricted open-shell Hartree−Fock calculations (ROHF) were carried out on possible low-lying triplet and quintet states of the neutral molecules as well as on the positive ions. Geometries of the closed-shell neutral species were computed using gradient optimization methods. All of the calculations utilized Gaussian 92.[34] The geometries of the neutral species were assumed for the calculations on the excited states and positive ions. In addition, second-order Moller−Plesset MP2 calculations,[35] or ROMP2 calculations for open-shell systems, were carried out for selected states to estimate the effects of electron correlation. The inner 4s and 4p electrons on Nb and 1s orbitals on C were not excited in these calculations.

4. Results and Discussion

A. Collisional Activation. $Nb_4C_4^+$ was found to be quite rugged, requiring the use of high-energy collisions (>50 eV center-of-mass frame) under conventional single-excitation CID conditions[30] to cause fragmentation. $Nb_4C_4^+$ dissociates through the loss of C, Nb, and NbC (Figure 2) to generate a combination of fragments including $Nb_3C_3^+$, $Nb_2C_2^+$, and Nb^+. $Nb_4C_3^+$ and $Nb_3C_4^+$ were also observed in minor amounts. At high energies, Nb^+ is the dominant product. These results are in accordance with photodissociation experiments.[22] The neutral NbC losses observed for $Nb_4C_4^+$ are consistent with a cubic structure containing Nb−C covalent bonds, as described below in the theoretical calculations.

B. Structure and Properties of Nb_4C_4 and $Nb_4C_4^+$. The geometry of neutral Nb_4C_4 corresponding to a cubic unit of the NaCl-type lattice was obtained assuming T_d symmetry at the SCF (Hartree−Fock) level. The geometrical parameters derived are summarized in Table 1. The resulting structure (shown in Figure 3) is a distorted cubic form, trigonal unit cell structure, with Nb−C bond lengths of 2.013 Å and Nb−C−Nb bond angles of 94.8° compared with the ideal cubic angle of 90°.

(34) Gaussian 92, Revision B: Frisch, M. J.; Trucks, G. W.; Head-Gordon, M.; Gill, P. M. W.; Wong, M. W.; Foresman, J. B.; Johnson, B. G.; Schlegel, H. B.; Robb, M. A.; Replogle, E. S.; Gomperts, R.; Andres, J. L.; Raghavarachari, K.; Binkley, J. S.; Gonzalez, C.; Martin, R. L.; Fox, D. J.; Defrees, D. J.; Baker, J.; Stewart, J. J. P.; Pople, J. A.; Gaussian, Inc.: Pittsburgh, PA, 1992.

(35) Pople, J. A.; Seeger, R.; Krishnan, R. *Int. J. Quantum Chem. Symp.* **1977**, *11*, 149.

Table 1. Selected Geometrical Parameters for Nb_4C_4 and Nb_4C_2

Nb_4C_4		Nb_4C_2	
	Bond Distances (Å)		
Nb−C	2.013	Nb1−C6	2.013
		Nb3−C6	2.086
Nb−Nb	2.964	Nb1−Nb3	2.717
C−C	2.719	Nb1−Nb2	2.855
		Nb3−Nb4	2.864
	Bond Angles (deg)		
Nb−C−Nb	94.8	Nb1−C6−Nb2	90.3
C−Nb−C	85.0	Nb1−C6−Nb3	83.0
		Nb1−Nb3−Nb2	63.4

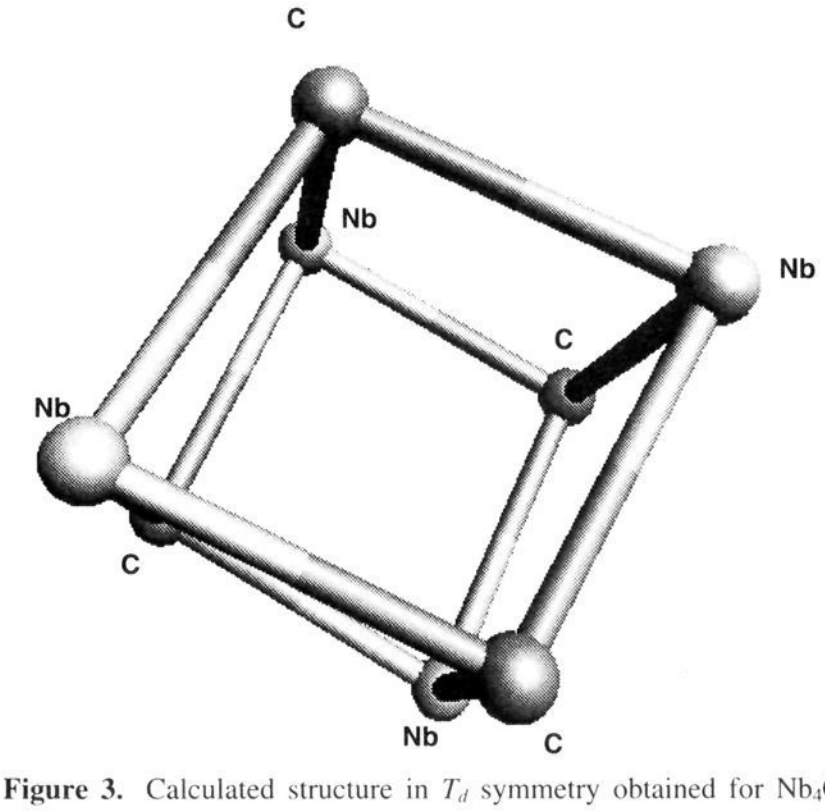

Figure 3. Calculated structure in T_d symmetry obtained for Nb_4C_4 from *ab initio* calculations.

The Nb_4C_4 molecule with this geometry has a closed-shell electronic structure with a configuration

$$(1a_1)^2(1t_2)^6(2a_1)^2(1e)^4(2t_2)^6(1t_1)^6(3t_2)^6(2e)^4$$

for the 36 valence electrons of the species. The lowest a_1 and t_2 levels correspond to 2s lone pairs on the C atoms, and the next five levels comprise the 12 Nb−C skeletal bonding orbitals of the cluster. The highest 2e level represents nonbonding 4d orbitals on the metal atoms. Such a closed-shell structure would not be expected to undergo Jahn−Teller distortions to lower symmetries than T_d. A similar situation would be expected for species such as Zr_4C_4 and Y_4N_4 with four less valence electrons. Such species would be expected to have similar stabilities since they share a common bonding framework.

The possible roles of these 2e nonbonding electrons will be revisited in Sections F and G, where reactions of the cluster with H_2O and CH_3OH yield products of the form $Nb_4C_4X_2^+$, X = OH and OCH_3. On the basis of the previous discussion, one might anticipate that up to 4 electrons could be removed from the cluster without disrupting the Nb−C skeletal bonds.

The lowest unoccupied orbitals are $4t_2$ and $3a_1$ and they give rise to various excited state multiplets. Two representative states have been examined: a triplet state with configuration $(2e)^3(4t_2)^1$ and a quintet state with configuration $(2e)^2(4t_2)^2$. The results are summarized in Table 2. At the SCF level these states appear to lie slightly below the closed-shell ground state, but when electron correlation effects are included at the MP2 level, the high-spin quintet state is destabilized by 25 kcal/mol and now lies above the closed-shell state.

Table 2. Relative Energies of Electronic States of Nb_4C_4 and Nb_4C_2 and Their Positive Ions[a]

state		E_{rel} (kcal/mol)		total energy (au)	
		HF	MP2	HF2	MP2
Nb_4C_4					
$S=0$	$(2e)^4$	0	0	−373.916 323	−376.017 205
$S=1$	$(2e)^3(4t_2)^1$	−6.2		−373.926 222	
$S=2$	$(2e)^2(4t_2)^2$	−12.3	+13.2	−373.935 963	−374.996 242
$Nb_4C_4^+$					
$S=1/2$	$(2e)^3$	88.8		−373.774 747	−374.876 017
$S=3/2$	$(2e)^2(4t_2)^1$	90.7		−373.771 713	
Nb_4C_2					
$S=0$	$(6a_1)^2$	0	0	−298.164 904	−299.044 928
$S=1$	$(6a_1)^1(5b_2)^1$	+17.0		−298.137 738	
$Nb_4C_2^+$					
$S=1/2$	$(6a_1)^1$	115.4		−297.980 951	−298.919 588
Nb atom					
$S=5/2$	$(5s)^1(4d)^4$			−55.679 44	−55.687 134
Nb^+ ion					
$S=2$	$(4d)^4$	137.5 [158.4][36]		−55.460 27	
$S=2$	$(4d)^3(5s)^1$	146.4 [165.8][36]		−55.445 95	
C atom					
$S=1$	$(2s)^2(2p)^2$			−37.676 866	−37.700 920

[a] Calculations for all states are reported using the ground state geometry of the neutral molecules.

For the $Nb_4C_4^+$ ion, removal of an electron from Nb_4C_4 results in a doublet state with configuration $(2e)^3$. Such a degenerate state would be expected to undergo Jahn−Teller distortions to lower symmetries than T_d. The scope of the present investigation has been limited to studies of "vertical" ion states at the neutral ground state geometry. An excited ion state arises from promotion of an electron in the 2e orbital to form the quartet state $(2e)^2(4t_2)^1$. At the SCF level, both states are predicted to be quite close in energy (Table 2).

The low-lying virtual $4t_2$ and $3a_1$ orbitals represent "σ-acceptor" orbitals and are oriented radially outward from the four Nb atoms. These unoccupied orbitals could be used in forming coordinative bonds with non-oxidizing ligands to form $Nb_4C_4(L)_m$ species, where at most four such ligands could be accommodated by these acceptor orbitals. This is apparently realized in the case of L = CH_3CN, as discussed more extensively in Section I where experimental results on coordination chemistry are presented.

Finally, to provide some calibration of the calculated ionization energies, the energies for the low-lying states of Nb and Nb^+ are given in Table 2 along with experimental values[36] at the Hartree−Fock level. Such energies are underestimated by about 20 kcal/mol (or nearly 1 eV) at this level for these open-shell systems. The calculated and experimental ionization energies (in eV), averaged over spin−orbit components, are 5.96 (6.87) and 6.35 (7.19) respectively for the lowest $4d^4$ and $5s^1$-$4d^3$ multiplets.

C. Reactivity with Oxygen. $Nb_4C_4^+$ reacts with a static pressure of oxygen at $\sim 7.2 \times 10^{-8}$ Torr via reaction 1 to generate $Nb_4C_2^+$ and, presumably, 2CO. An analogous oxidative decomposition process has been observed for the $V_8C_{12}^+$ metallo-carbohedrene cluster.[16] It is also found that a very small amount of oxidation product, $Nb_4C_3O^+$, is formed through reaction 2. The reaction of oxygen with $Nb_4C_4^+$ to generate 2CO

$$Nb_4C_4^+ + O_2 \rightarrow Nb_4C_2^+ + 2CO \quad (1)$$

$$\rightarrow Nb_4C_3O^+ + CO \quad (2)$$

may indicate that the carbon atoms eliminated as CO are in adjacent positions on the cluster in analogy to metallo-carbohedrenes. Based on the 2×2×2 structure, however, the oxidation process likely proceeds through the homolysis of the oxygen−oxygen double bond and a subsequent elimination of two carbon monoxides from the cluster. In contrast to the formation of $V_8C_N^+$ (N is even and <12), arising from the reaction of $V_8C_{12}^+$ with O_2, however, collisionally cooled $Nb_4C_2^+$ does not undergo further oxidative decomposition to form Nb_4^+. Formation of 2CO from C_2 and O_2 is ~10 eV exothermic.[37] In a related study in our laboratory, Nb_4^+ was found to react with C_2H_4 to generate $Nb_4C_2^+$, which subsequently reacts to yield $Nb_4C_4^+$ and $Nb_4C_4H_2^+$.[38] Taken together these results suggest that 8 eV < $D(Nb_4C_2^+-C_2)$ < 10 eV and $D(Nb_4^+-C_2)$ > 10 eV.

D. Properties of Nb_4C_2. The formation of $Nb_4C_2^+$ in the above reactions with O_2 prompted us to investigate the properties of Nb_4C_2 and its ion at the same level as the Nb_4C_4 calculations. The geometry obtained for a closed-shell Nb_4C_2 species is shown in Figure 4, and the geometrical parameters are given in Table 1. C_s symmetry was assumed in the optimization, but the resultant structure has essentially C_{2v} symmetry, corresponding to a bicapped tetrahedron. The calculated bond lengths in C_s symmetry differ from one another by only 0.002 Å for those bonds that are equivalent in C_{2v} symmetry. The Nb−C bond lengths are similar to those found in Nb_4C_4, and the Nb−C−Nb bond angle is essentially 90°. The electronic structure of Nb_4C_2 is

$$...(3b_2)^2(2b_1)^2(5a_1)^2(2a_2)^2(4b_2)^2(6a_1)^2$$

for the highest 6 MOs in C_{2v} symmetry. For the 14 MOs describing the 28 valence electrons, 2 correspond to the 2s lone-pair orbitals of C, and the remaining 12 describe the 6 Nb−C and 6 Nb−Nb skeletal bonds of the cluster. Although one should not interpret the schematic structure in Figure 4 too literally, the symmetries of the occupied orbitals correspond to what one would expect from two 2s orbitals on C (a_1, b_2), six Nb−C (two a_1 and b_2, one b_1 and a_2) orbitals, and six Nb−Nb (three a_1, one each of a_2, b_2, and b_1) orbitals. A triplet state

(36) *Atomic Energy Levels*; Moore, C. E., Ed.; 1952; NBS Circular 476, pp 216−221.

(37) Lias, S. G.; Bartmess, J. E.; Liebman, J. F.; Holmes, J. L.; Levin, R. D.; Mallard, W. G. *J. Phys. Chem. Ref. Data* **1988**, *17*, Suppl. 1.

(38) Jiao, C. Q.; Freiser, B. S. *J. Phys. Chem.* In press.

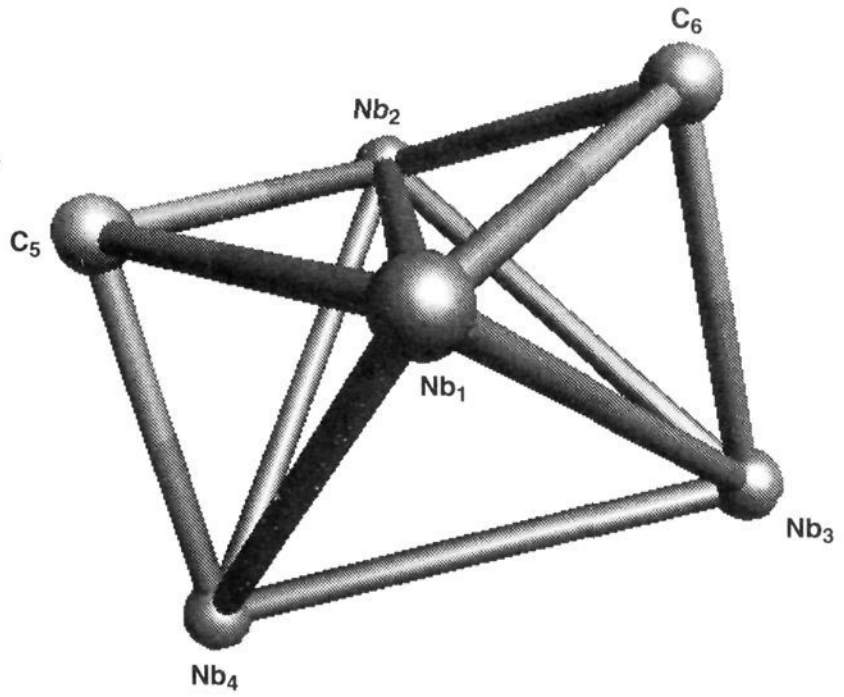

Figure 4. Calculated structure having C_{2v} symmetry obtained for Nb_4C_2 from *ab initio* calculations.

corresponding to $(6a_1)^1(5b_2)^1$ was also investigated and found to lie above the singlet state at the SCF level (Table 2). The $Nb_4C_2^+$ ion with a configuration corresponding to removing one electron from the $6a_1$ orbital was also calculated. The calculated vertical ionization potentials of Nb_4C_4 and Nb_4C_2 are 3.8 and 3.4 eV, respectively, at the MP2 level. While the structure in Figure 4 represents one stable form, there remains the possibility of other geometric structures that are stable regions on the potential hypersurface.

The Mulliken population analysis yields the following results for effective charges (q) and valence populations: in Nb_4C_4 $q = +0.587$ and $(s,p)^{0.827}$ $d^{3.586}$ orbital populations for Nb and $q = -0.587$ and $s^{1.582}$ $p^{3.005}$ for C; in Nb_4C_2 $q = +0.488$ and $(s,p)^{0.941}$ $d^{3.571}$ for $Nb_{1,2}$, $q = +0.216$ and $(s,p)^{1.174}$ $d^{3.610}$ for $Nb_{3,4}$, and $q = -0.705$ and $s^{1.697}$ $p^{3.008}$ for C.

E. Stabilities and Reactivities of Nb_4C_4 and Nb_4C_2. In an attempt to understand the observed reactivity of $Nb_4C_4^+$ with O_2 to form $Nb_4C_2^+$, the overall stabilities of Nb_4C_4, Nb_4C_2, and their ions were examined. The present results must be viewed as qualitative, however, even though a flexible basis set has been used, since methods to obtain accurate thermochemical properties for organometallic species are in a considerably less refined state than those for organic species. One possible measure of the relative stability of these species is a comparison of the relative binding energies/atom—calculated to be 115 and 93 kcal/mol at the MP2 level for Nb_4C_4 and Nb_4C_2, respectively, for a relative difference of 22 kcal/mol—indicating a somewhat greater stability of the Nb_4C_4 building block of larger cubic Nb_xC_y species.

For the reactions of the neutral and ionic species with O_2

$$Nb_4C_4 + O_2 \rightarrow Nb_4C_2 + 2CO$$

$$Nb_4C_4^+ + O_2 \rightarrow Nb_4C_2^+ + 2CO$$

both reactions are computed to be nearly thermoneutral: +4.8 kcal/mol for the neutral reaction and −5.1 kcal/mol for the ion reaction at the MP2 level. Although one cannot expect very quantitative thermochemistry from such calculations for reactions on molecules of this size, there does not appear at this point to be a great qualitative difference between the reactivities of the neutral and ionic species. These results do not include zero-point contributions and do not allow geometrical relaxation effects for the positive ions. As another calibration point, the thermochemistry of the neutral reaction was calculated using a more accurate 6−31G* basis for C with a resultant reaction energy of −2.8 kcal/mol.

Scheme 1

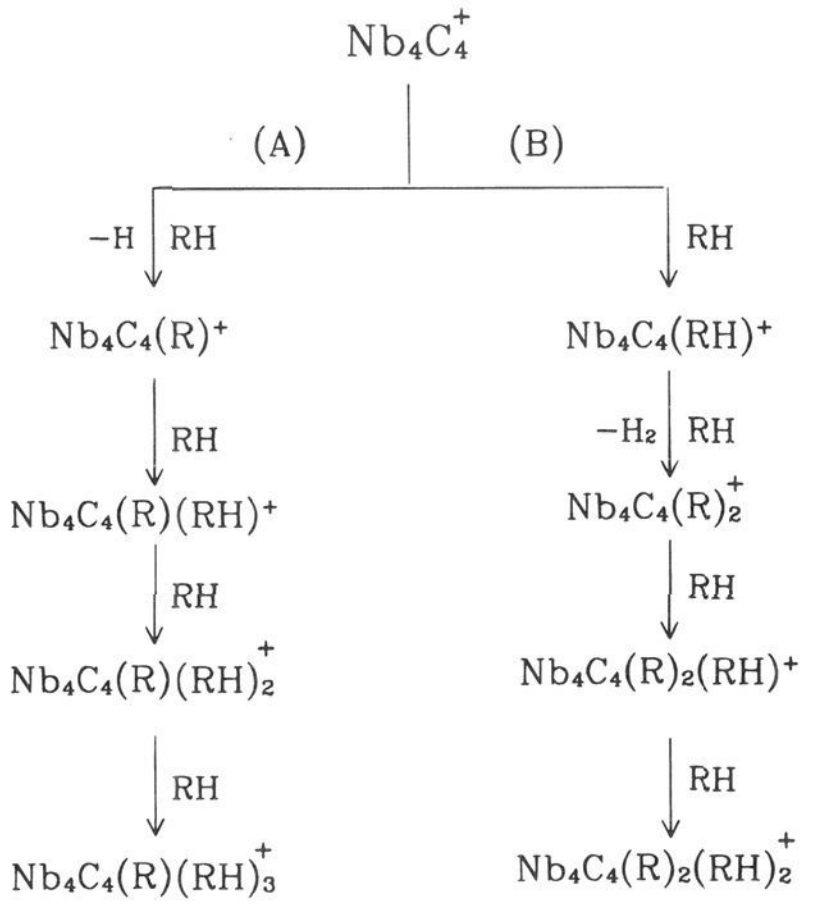

R = OH, OCH_3

F. Reactivity with Water. Two competitive pathways are found for the reactions of $Nb_4C_4^+$ with H_2O (1.7×10^{-7} Torr) which are dependent on the pressure of the background argon cooling gas. As shown in Scheme 1, pathway A, in the absence of argon the reaction proceeds predominantly by initial OH abstraction followed by sequential addition of H_2O leading to the buildup of $Nb_4C_4(OH)(H_2O)_3^+$. In the presence of argon cooling gas, however, the chemistry changes dramatically to pathway B. There is an initial addition of H_2O, and reaction with the second water proceeds by elimination of H_2 yielding, presumably, $Nb_4C_4(OH)_2^+$. This species then reacts further to coordinate an additional 2 waters to yield $Nb_4C_4(OH)_2(H_2O)_2^+$, *Figure 5. As expected, the overall reaction proceeds more* rapidly when the ions are cooled in the presence of the Ar background gas. Analogous decomposition reactions accompanied by the loss of H_2 have been observed for $V_8C_{12}^+$ and other metal clusters with selected ligands (i.e. H_2O, D_2O, NH_3).[16,39]

Reaction pathways for this system were determined initially using double resonance to continuously eject a reactant ion[40] and verified by isolating the reactant ion and monitoring its further reactions. For example, $Nb_4C_4OH^+$ was isolated and its subsequent condensation reactions with H_2O were then monitored, confirming pathway A. In addition, an alternative experiment, SORI,[41] which is used to slowly increase the internal energy of an ion through soft collisions, was performed by varying the excitation time on $Nb_4C_4^+$. Under these conditions, only the products from pathway A are observed. These

(39) Riley, S. J. In *Metal−Ligand Interactions: From Atoms, to Clusters, to Surfaces*; Salahub, D. R., Russo, N., Eds.; NATO ASI Series C 378; The Netherlands, 1992; pp 17−34.

(40) Comisarow, M. B.; Grassi, V.; Parisod, G. *Chem. Phys. Lett.* **1978**, *57*, 413.

(41) Gautheir, J. W.; Trautman, T. R.; Jacobson, D. B. *Anal. Chim. Acta* **1991**, *246*, 211.

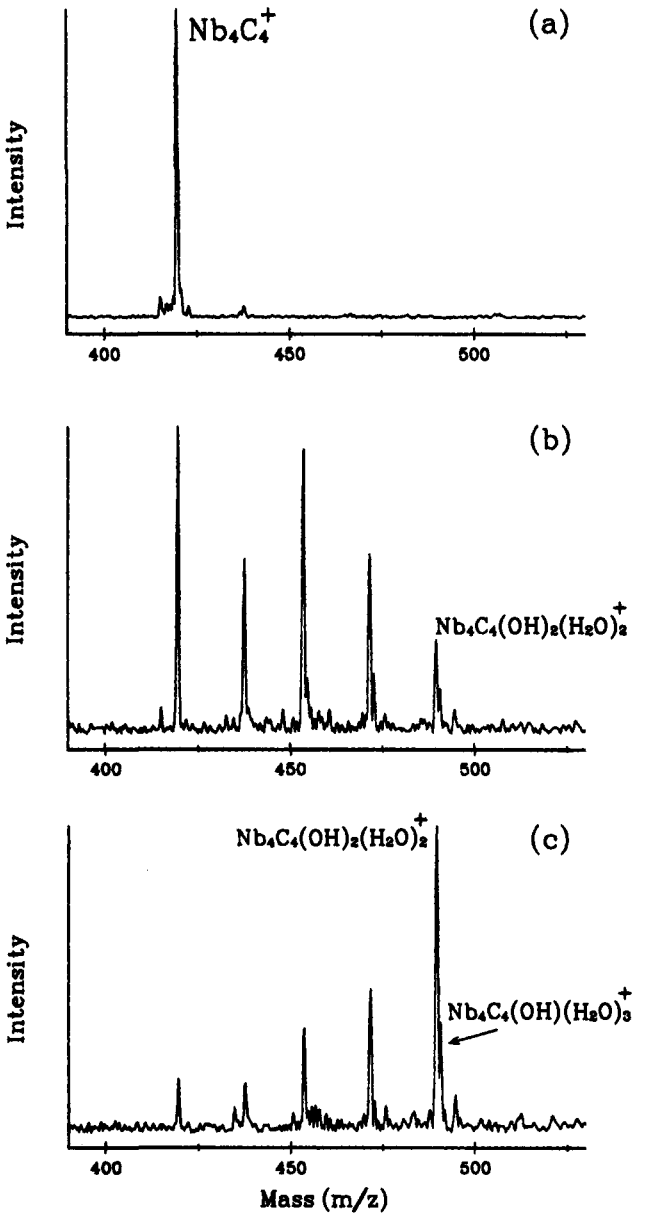

Figure 5. Reaction of $Nb_4C_4^+$ with H_2O at increasing reaction time: (a) isolated $Nb_4C_4^+$; (b) 6 s reaction time; (c) 10 s reaction time.

experimental results indicate that initial OH abstraction is an endothermic process, i.e., $D(Nb_4C_4^+-OH) < D(H-OH) = 119$ kcal/mol.[37]

The previous discussion on the electronic structure of Nb_4C_4 would lead one to anticipate that the 4 nonbonding electrons in the highest e molecular orbital could participate in chemistry without disrupting the skeletal Nb–C bonding framework of the cluster. Similarly, 3 nonbonding electrons are available for the $Nb_4C_4^+$ ion. Some indication of this is provided by the above experimental observations that, following the addition of the first H_2O molecule, elimination of H_2 occurs upon reaction with the second H_2O to form $Nb_4C_4(OH)_2^+$. The $Nb_4C_4(OH)_2^+$ can be represented by a Nb_4C_4 core that has formally ionized three electrons—two for the OH groups and one for the positive ion. The fact that the next two H_2O molecules simply complex may indicate that further oxidation is not energetically favorable.

One would expect the $Nb_4C_4(OH)_2^+$ species to have the OH groups bound to the metal sites both from the standpoint of the net positive charge already on the Nb atoms (based on the preceding population analysis) and from the consideration that the nonbonding 2e orbitals are primarily metal 4d in character. Similarly, any H_2O ligands coordinated to the cluster should

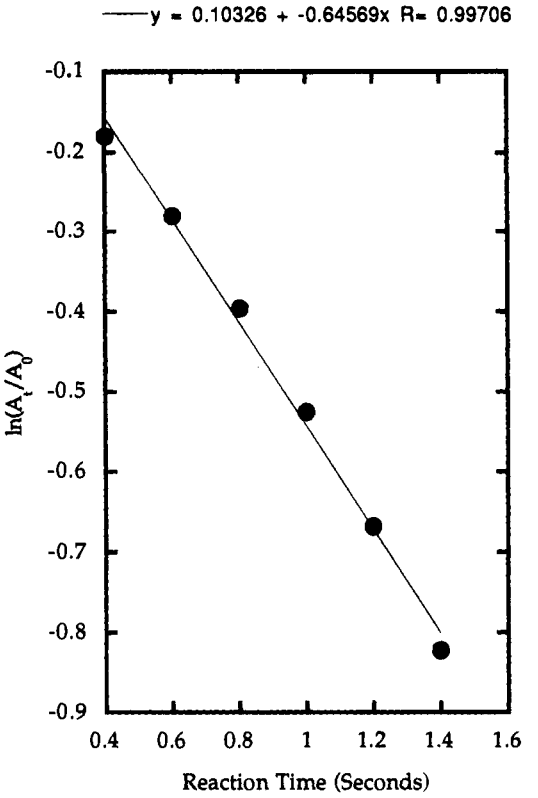

Figure 6. Pseudo-first-order plot of the reaction of $Nb_4C_4^+$ with methanol at 2.3×10^{-7} Torr.

also be bound to the metal by virtue of the 4 empty acceptor orbitals (Section B), as well as from electrostatic bonding.

G. Reactivity with Methanol. In analogy to the reactions with H_2O, methanol (2.3×10^{-7} Torr) is also observed to react via two pathways, Scheme 1. In the absence of collision gas or by applying SORI to $Nb_4C_4^+$, A is the dominant pathway observed in which OCH_3 is first abstracted followed by sequential solvation yielding $Nb_4C_4(OCH_3)(CH_3OH)_3^+$. In the presence of Ar, pathway B grows in importance. In analogy to the H_2O reaction, attachment of the first methanol is followed by H_2 elimination in the secondary reaction to form, presumably, $Nb_4C_4(OCH_3)_2^+$. This ion then sequentially reacts with methanol by addition to form $Nb_4C_4(OCH_3)_2(CH_3OH)_2^+$. Pathway A, which begins by attachment of OCH_3, however, remains the dominant process even in the presence of Ar cooling gas. Thus, unlike H_2O, this process may be exothermic for methanol, probably because of the considerably lower O–H bond strength in CH_3OH. The abstraction of an OCH_3 from methanol indicates that $D°(Nb_4C_4^+-OCH_3) \geq D°(H-OCH_3) = 104$ kcal/mol.[37] Interestingly, there is no evidence that $Nb_4C_4^+$ attacks the CH_3-OH bond, despite its being considerably weaker (~92 kcal/mol).[37]

H. Reaction Kinetics for Water and Methanol. Pseudo-first-order kinetics are observed for the reactions of $Nb_4C_4^+$ with H_2O and CH_3OH in the presence of Ar (Figures 6 and 7), indicating, but not unequivocally, that the $Nb_4C_4^+$ species are thermalized and consist of a single isomeric structure. The slopes of the pseudo-first-order plots are used with the estimated pressures to obtain the observed rate constants, k_{ob}, for H_2O and CH_3OH of 8.7×10^{-11} and 4.7×10^{-11} cm^3 molecule^{-1} s^{-1}, respectively. The reaction efficiencies for H_2O and CH_3OH are calculated by comparing k_{ob} to the Average Dipole Orientation rate constant, k_{ADO}, which is an estimate of collision frequency.[42] The parameters for each molecule, such as the polarizability (α), the dipole moment (μ_D), the reduced mass (μ), and the dipole locking parameter (c) which is a function of

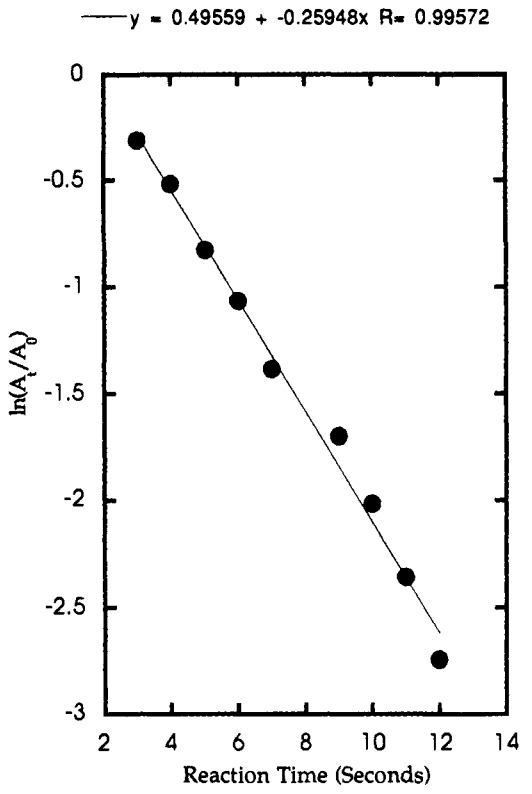

Figure 7. Pseudo-first-order plot of the reaction of $Nb_4C_4^+$ with water at 1.72×10^{-7} Torr.

Table 3. Parameters Used To Calculate k_{ADO} for Water and Methanol

reagent	α (Å^3)[43]	μ_D (D)[44]	c parameter[42]	μ (daltons)
water	1.45	1.88	0.251	17.26
methanol	3.23	1.77	0.220	29.73

Table 4. Rate Constants and Calculated Reaction Efficiencies for the Reactions of $Nb_4C_4^+$ with Water and Methanol

reagent	k_{ob}	k_{ADO}[42]	reaction efficiency
water	8.66×10^{-11}	2.18×10^{-9}	3.9
methanol	4.67×10^{-11}	1.7×10^{-9}	2.7

$\mu_D/\alpha^{1/2}$, used for calculating k_{ADO} are listed in Table 3. k_{ob}, k_{ADO}, and reaction efficiencies (k_{ob}/k_{ADO}) are summarized in Table 4. The reactions are found to be 3.9% and 2.7% efficient for water and methanol, respectively. While bimolecular condensation reactions can be expected not be very efficient, the low efficiency observed for OCH_3 abstraction from methanol suggests that the reaction is near thermoneutral and, perhaps, slightly (up to 5 kcal/mol) endothermic. Therefore, we assign $D(Nb_4C_4^+-OCH_3) \sim D(CH_3O-H) = 104$ kcal/mol.

(42) (a) Su, T.; Bowers, M. T. *Int. J. Mass Spectrom. Ion Phys.* **1973**, *12*, 347. (b) Su, T.; Bowers, M. T. *Int. J. Mass Spectrom. Ion Phys.* **1975**, *17*, 211.

(43) Miller, K. J. *J. Am. Chem. Soc.* **1990**, *112*, 8533.

(44) *Tables of Experimental Dipole Moments*; McClellan, A. L., Ed.; El Cerrito, CA, 1974; Vol. 2, pp 26, 42.

I. Study of Coordination. The coordinative saturation of the cluster was studied in an attempt to determine whether the 4 niobium atoms are in equivalent sites. This was done by "titrating" the metal atoms with the nucleophile CH_3CN. $Nb_4C_4^+$ was indeed found to coordinate up to a maximum of 4 CH_3CN. This is entirely consistent with the electronic structure analysis (Section B) where the presence of four low-lying σ-acceptor orbitals on the Nb centers was noted that would favor coordination with lone pairs of σ-donor ligands such as CH_3CN. These studies, however, were also complicated by the presence of background H_2O and the formation of various combination products, such as $Nb_4C_4(CH_3CN)_xH_2O^+$ and $Nb_4C_4(CH_3CN)_x(OH)_2^+$ with $x = 1-3$. Interestingly, two products were observed to exhibit a total coordination number of 5, $Nb_4C_4(CH_3CN)_2(OH)_2H_2O^+$ and $Nb_4C_4(CH_3CN)_3(OH)_2^+$. These results suggest that such titration experiments to determine the number of exposed metal atoms (based on 1:1 ligand-to-metal coordination) may be misleading, considering as an extreme Nb^+ itself which coordinates multiple ligands.[45] Alternatively, the results might suggest the interesting possibility that OH and CH_3CN can coordinate different sites.

5. Summary

$Nb_4C_4^+$ is found to be reactive with O_2, undergoing oxidative decomposition to form $Nb_4C_2^+$. Taken together with other experiments, this result yields the bond energy brackets 8 eV $< D(Nb_4C_2^+-C_2) <$ 10 eV. $Nb_4C_4^+$ is also found to react with water and methanol through the elimination of H_2 to form $(OH)_2$ and $(OCH_3)_2$ adducts, respectively, after which the reaction proceeds through solvation with two additional solvents. The ligand decomposition reaction via loss of H_2 is significant in representing a prototype to such reactions proceeding on heterogeneous catalysts. An intense peak corresponding to $Nb_4C_4(OCH_3)(CH_3OH)_3^+$ is also observed in the methanol reaction. The rate constants for the reactions with water and methanol are determined to be 8.7×10^{-11} and 4.7×10^{-11} cm^3 molecule^{-1} s^{-1}, respectively, which correspond to efficiencies of 3.9% and 2.7%. Taken in total, these results suggest $D(Nb_4C_4^+-OH) \leq D(H-OH) = 119$ kcal/mol and $D(Nb_4C_4^+-OCH_3) \sim D(H-OCH_3) = 104$ kcal/mol. The neutral Nb_4C_4 species is found to form a slightly distorted cubic structure corresponding to the smallest 2×2×2 building block of the larger cubic clusters, such as $Nb_{14}C_{13}$. Nb_4C_2 adopts a bicapped tetrahedron structure derived qualitatively from removing two carbons from the corners of the Nb_4C_4 cluster.

Acknowledgment is made by B.S.F. to the National Science Foundation (CHE-9224476) and to the Division of Chemical Sciences in the Office of Basic Energy Sciences in the United States Department of Energy (DE-FG02-87ER13766), and by P.J.H. to the Department of Energy (under Laboratory Directed Research and Development at Los Alamos) for supporting this research.

JA943127V

(45) Buckner, S. W.; MacMahon, T. J.; Byrd, G. D.; Freiser, B. S. *Inorg. Chem.* **1989**, *28*, 3511.